Available online at www.sciencedirect.com
SCIENCE DIRECT®
Protein Expression and Purification 43 (2005) 103–110
Protein Expression & Purification
www.elsevier.com/locate/yprep

Purification and in vitro characterization of the maltose-binding protein of the plant pathogen *Xanthomonas citri*

Andrea Balan [a], Cristiane Santos de Souza [a], Alexandre Moutran [a], Rita C. Café Ferreira [a], Christian Suarez Franco [a], Carlos Henrique I. Ramos [b], Luís Carlos de Souza Ferreira [a,*]

[a] *Departamento de Microbiologia, Instituto de Ciências Biomédicas II, Universidade de São Paulo, CEP 05508-000, Cidade Universitária, SP, Brazil*
[b] *Centro de Biologia Molecular Estrutural, Laboratório Nacional de Luz Síncrotron, Campinas, SP, Brazil*

Received 4 February 2005, and in revised form 16 March 2005
Available online 9 April 2005

Abstract

The uptake of maltose and maltodextrins in gram-negative bacteria is mediated by an ATP-dependent transport complex composed of a periplasmic maltose-binding protein (MBP) and membrane-associated proteins responsible for the formation of a membrane pore and generation of energy to drive the translocation process. In this work, we report the purification and in vitro functional analysis of MBP, encoded by the *malE* gene, of the plant pathogen *Xanthomonas citri*, responsible for the canker disease affecting citrus plants throughout the world. The *X. citri* MBP is composed of 456 amino acids, displaying a low amino acid identity (16% throughout the sequence) compared to the *Escherichia coli* K12 ortholog. The *X. citri malE* gene was cloned into a pET28a vector, and the encoded protein was expressed and purified by affinity chromatography as a His-tag N-terminal fusion peptide produced by the *E. coli* BL21 strain. Enhanced levels of soluble protein were achieved with static cultures kept overnight at 23 °C. Ability to bind immobilized amylose, the emission of intrinsic fluorescence and circular dichroism spectra indicated that the purified recombinant protein preserved both conformation and biological activity of the native protein. The availability of the recombinant MBP will contribute to the functional and structural analysis of the maltose and maltodextrin uptake system of the plant pathogen *X. citri*.

Keywords: Maltose-binding protein; MPB; *malE*; *Xanthomonas citri*

Maltose- or maltodextrin-binding proteins (MBP)[1] are produced by and accumulated in the periplasm of several gram-negative bacterial species, where they interact with high affinity to substrates such as the disaccharide maltose, as well as with longer linear maltodextrins or even cyclodextrins, before uptake to the cell interior [1,2]. In *Escherichia coli* K12, the active transport of maltose and maltodextrins depends upon MBP and an ATP-dependent membrane-associated transport system comprised of two integral membrane proteins (MalF and MalG) and two copies of an ATP-hydrolyzing subunit (MalK) [3]. Similar to other ABC-type transport binding components, MBP or MalE typically contains two nearly symmetrical lobes separated by a hinge region where the substrate-binding site lies [4]. After binding, the protein undergoes a conformational change as a direct result of the lobes bending and twisting toward each other leading to substrate enclosure [4–7]. MBPs also participate in maltose taxis after interaction of the bound complex with the periplasmic portion of the Tar protein [8].

MBP orthologs from different gram-negative and gram-positive bacteria, such as the hyperthermophile *Pyrococcus furiosus* and *Themococcus litoralis*, have been cloned and expressed in *E. coli* K12 aiming to

* Corresponding author. Fax: +55 11 30917354.
E-mail address: lcsf@usp.br (L.C. de Souza Ferreira).
[1] *Abbreviations used:* MBP, maltose-binding protein; CD, circular dichroism.

1046-5928/$ - see front matter © 2005 Elsevier Inc. All rights reserved.
doi:10.1016/j.pep.2005.03.018

define the three-dimensional structures and physiological features [9–11]. However, no ortholog derived from plant-associated bacteria has been reported so far. In such cases, identification, expression, and purification of components pertaining to the uptake transport system followed by functional and structural analyses represent essential steps toward defining the physiological and functional role of the uptake system in regard to the nutritional strategies of the bacterial pathogen.

The genus *Xanthomonas* comprises a diverse group of bacterial phytopathogens, belonging to the γ-subdivision of the proteobacteria. *X. citri* is the causative agent of the citrus canker, which affects most commercial citrus cultivars, resulting in significant economic losses worldwide [12]. The definition of the complete genome sequences of *X. citri* revealed that approximately 4% of the structural genes are devoted to the synthesis of ATP-dependent transport system components, including ABC-transporters [13]. Ability to use sugars and polysaccharides represents an important feature of bacterial species living in close association with plant hosts. Nonetheless, no previous attempts to identify and characterize ABC-transporters dedicated to the transport of maltose and maltodextrins in *X. citri* have been reported. In this work, we report the identification and purification of the *X. citri* MBP ortholog. The recombinant protein was expressed in *E. coli* BL21(DE3) and its functionality evaluated under in vitro conditions.

Materials and methods

Strains and plasmids

All strains and plasmids used in this work are listed in Table 1.

Cloning of the malE X. citri gene

The nucleotide sequence encoding the mature *X. citri* MBP (without the first 57 base pair encoding the 19 amino acid long signal peptide) was amplified by PCR (forward primer, 5′ GCAGGTCATATGGGATGCGA 3′ and reverse primer, 5′ CCGGAAGCTTTCATCGTGC 3′) using Platinum high fidelity *Taq* polymerase (Invitrogen) using standard amplification conditions: an initial step of 5 min at 95 °C, 1 min at 95 °C; followed by 25 cycles of 1 min at 49.4 °C, 2 min at 72 °C; and followed by a final extension at 72 °C for 10 min. The forward primer included a *Nde*I site, and the reverse primer a *Hin*dIII site (underlined). The resulting amplified fragment, with a total length of 1311 nucleotides, was first cloned into the vector pGEM T-Easy (Promega) using standard cloning conditions. After transformation of *E. coli* DH5α cells and screening of recombinant colonies, a recombinant plasmid, named pGEMMalE, was selected, amplified, and cleaved with *Nde*I and *Hin*dIII enzymes (Invitrogen) to release the 1311 kbp fragment, which was purified from agarose gels and subsequently cloned into the expression vector pET28a (Novagen), previously treated with *Nde*I/*Hin*dIII. Transformation efficiencies of approximately 10^7 c.f.u./μg DNA were routinely achieved with chemically competent *E. coli* DH5α cells. One recombinant colony, selected out of 10 chosen colonies, was subjected to restriction analysis and nucleotide sequencing. The recombinant plasmid, named pETMalE, was further purified in larger quantities and transformed into the *E. coli* BL21(DE3) strain (Novagen). One recombinant clone chosen at random among a lawn of recombinant colonies was selected for further analysis of protein expression and purification. The recombinant *X. citri* MBP was expressed as a cytoplasmic protein with a His_6-tag genetically fused at the N-terminal end (HT-MBP).

Table 1
Strains and plasmids used in this work

	Reference or gene ID
Strains	
E. coli DH5α	Laboratory stock
E. coli BL21(DE3)	Invitrogen
X. citri 306	1156381
Plasmids	
pGEM T-easy	Promega
pGEMMalE	This work
pET28a	Novagen
pETMalE	This work

Computational analysis

The nucleotide and corresponding amino acid sequences of the *X. citri malE* gene (gene ID 1156381) were made available by the *Xanthomonas* project (http://genoma4.iq.usp.br/xanthomonas) and retrieved from the GenBank (Accession No. AE011868). Search of MBP ortholog sequences was first carried out using the KEGG2 program of the Bioinformatics Center Institute for Chemical Research Kyoto University (www.genome.jp). The alignments of MBP amino acid sequences were carried out using the BLASTP, available at the National Center of Biotechnology Information server (http://www.ncbi.nlm.nih.gov/BLAST) and ClustalW (www.ebi.ac.uk/clustalw/). Prediction of signal peptide and transmembrane sequences was determined with SignalP and DAS programs, respectively (http://www.cbs.dtu.dk/services/SignalP/, and http://www.sbc.su.se/~miklos/DAS/). Protein parameters of the *X. citri* MBP were calculated with application of programs available at the Expasy Molecular Biology Server (http://www.au.expasy.org/). Definition of conserved structural domains was carried out with the Conserved Domain Search program available at NCBI (http://

www.ncbi.nlm.nih.gov/Structure/cdd/wrpsb.cgi), as previously reported by Marchler-Bauer and Bryant [14]. The MBP sequences reported in Fig. 1 are those derived from *X. campestris*, *Xylella fastidiosa*, *Salmonella typhimurium*, *Shigella flexneri*, *Yersinia pestis*, *Erwinia carotovora*, *E. coli*, *Pyrococcus furiosus*, *Thermococcus litoralis*, and *Alicyclobacillus acidocaldarius*.

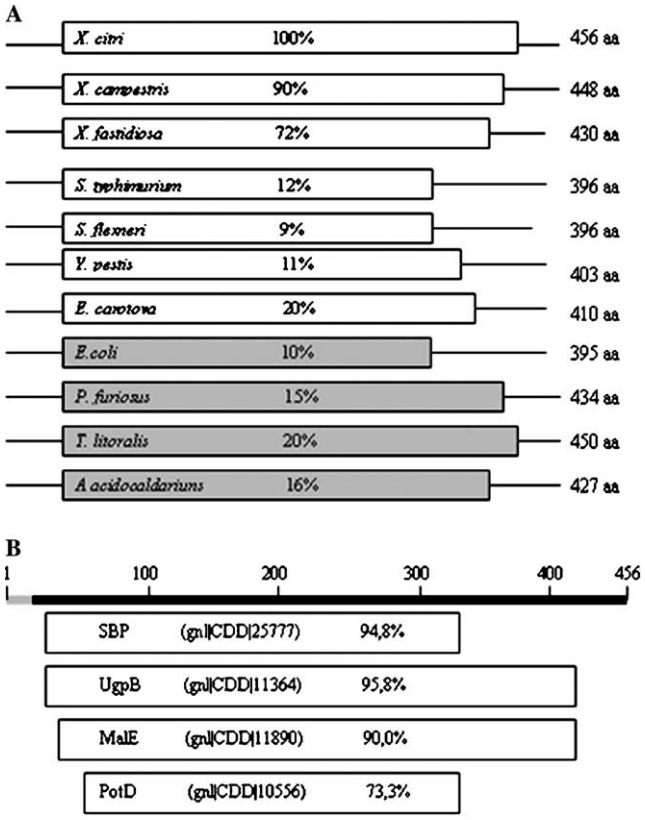

Fig. 1. Computational analysis of *X. citri* MBP comprising sequence alignments and definition of functional and structural domains. (A) Amino acid identity shared by different bacterial MBPs in relation to the *X. citri* protein. The open boxes indicate the amino acid identity values (expressed as percent of the total amino acid sequence of *X. citri* MBP) of MBP orthologs expressed by different bacterial species. The total numbers of amino acids of the MBPs expressed by the different bacterial species are indicated in the left side of the figure. Boxes in gray represent MBPs with solved structure available at the Protein Data Bank. (B) Analysis of conserved structural and functional domains of *X. citri* MBP based on comparison with other periplasmic binding proteins, as determined with the Conserved Domain Search program. The bar and numbers on the top of the figure (signal peptide in gray, mature sequence in black) refer to the size in amino acids of the *X. citri* MBP. The open boxes indicate the classes of binding proteins sharing conserved functional and structural domains with *X. citri* MBP, as indicated: SBP, bacterial extracellular solute-binding proteins; UgpB, sugar-binding proteins; MBP, maltose-binding proteins; and PotD, spermine/putrescine-binding proteins. The accession numbers of each protein class sharing similarity with *X. citri* MBP are indicated, as well as the calculated similarity values, expressed as percentages of *X. citri* MBP amino acid sequence used in the analysis (SBP, 330 residues; UgpB, 403 residues; MalE, 420 residues; and PotD, 363 residues).

Protein expression and purification

Cultures of the recombinant *E. coli* BL21(DE3) strain carrying pETMalE were grown aerobically in Erlenmeyer flasks containing LB or M9 medium with 50 μg/mL kanamycin until mid-log phase (OD_{600} 0.5–0.6) before inducer adding (0.1 mM IPTG). The cultures were induced aerobically (200 rpm) either for 2 or 4 h or statically overnight at different temperatures (23, 28, and 37 °C). Optimal expression levels as well as higher solubility levels were defined after evaluating different induction parameters including growth media, aeration, and temperature during the induction period. Cells were collected by centrifugation and stored at −20 °C for approximately 16 h before preparation of the cell extracts. Cell pellets from 1 L cultures were suspended in 10 mL Buffer 1 (10 mM Tris–Cl, pH 8.0, 100 mM NaCl, 0.5 mM PMSF, and 3 mM imidazole) and incubated with lysozyme (final concentration of 100 μg/mL) for 1 h in an ice bath. Cells were maintained in ice and sonically disrupted after 4 pulses of 20 s. in a Branson Digital Sonifier (Model 450), with 30% amplitude, followed by centrifugation at 18,000 rpm for 20 min to obtain the soluble and non-soluble cellular fractions. The HT-MBP was purified from soluble protein extracts after addition of a nickel-charged Sepharose (ProBond, Invitrogen) slurry (1 mL of resin for 15 mg of total protein) previously washed with two volumes of water and one volume of Buffer 1, and incubated for 1 h under mild agitation. The charged resin was transferred to a plastic column and washed with 10 volumes with Buffer 1 followed by washing with three volumes of Buffer 2 (Buffer 1 plus 20 mM imidazole). The bound HT-MBP was serially eluted with buffers with increasing imidazole concentrations (Buffer 3, 50 mM; Buffer 4, 100 mM; Buffer 5, 200 mM; and Buffer 6, 500 mM). Eluted HT-MBP-containing fractions were dialyzed with 50 mM Tris–Cl and 100 mM NaCl. Samples were concentrated with Ultrafree MWCO 10,000 centrifugal filters (Amicon Millipore) to a final concentration of 10 mg/mL. The eluted protein fractions were analyzed by SDS–PAGE using 12% acrylamide gels. Amylose-binding experiments were performed with purified HT-MBP in Buffer A (Tris 20 mM, pH 8.2, NaCl 50 mM, and 10 mM maltose) and amylose resin (England Biolabs). The protein was mixed with the resin at a ratio of 1 mL resin:3 mg protein and incubated for 1 h at room temperature. After two washes with Buffer A, the bound HT-MBP was eluted with Buffer A, which contained 150 mM maltose. All samples were analyzed by SDS–PAGE using 12.5% acrylamide gels stained with Coomassie blue. Protein concentration was determined spectrophotometrically using the Edelhoch method [15].

Circular dichroism

Experiments were performed with 10 μM MBP and 20 μM maltose in buffer Tris 20 mM, pH 8.2, NaCl 50 mM. Circular dichroism (CD) spectra were recorded using a JASCO J-820 spectropolarimeter equipped with a thermoelectric sample temperature controller (Peltier system). The data were recorded from 260 to 200 nm at 21 °C using a quartz cell (Helma) with a path length of 1.0 mm. To improve the signal-to-noise ratio, a total of 20 accumulations were taken for each spectrum with a speed of 20 nm/min at a resolution of 0.5 nm, responses of 1 s and bandwidth of 1.0 nm. Secondary structures were assigned using the DICROPROT program [16].

Fluorescence measurements

All fluorescence experiments were performed in 20 mM Tris–Cl, pH 8.2, 100 mM NaCl at 21 °C. Protein samples (1 μM) were incubated with maltose concentrations ranging from 1 to 9 μM before monitoring the emitted fluorescence on a Bowman Series 2 spectrofluorometer (AMINCO) set at an excitation wavelength of 295 nm. The fluorescence emission was recorded in wavelengths ranging from of 300 to 450 nm with spectral bandwidths of 2 nm. The fluorescence integer was calculated using the Origin software (Microcal), and the emission fluorescence center of mass (CM) was calculated with the following equation:

$$\mathrm{CM} = \sum v_i \mathrm{x}\ \mathrm{F}_i / \sum \mathrm{F}_i, \quad (1)$$

where v_i is the wavelength and F_i is the intensity at v_i [17].

Results

Identification of the X. citri malE gene and sequence similarity analysis with orthologs

The search of *X. citri malE* orthologs led to the identification of one open reading frame (GI:21108556, 1368 base pair) and another one in the closely related phytopathogen *X. campestris* (GI:998803, 1344 base pair). Both genes were annotated as *malE* and would be responsible for the codification of MBP in these bacterial species [14]. The *X. citri malE* gene encodes a putative protein with 456 amino acids, with a predicted signal peptide of 19 amino acids, while the *X. campestris malE* gene encodes a putative protein of 448 amino acids. Alignment of the *X. citri* MBP with different orthologs showed that the proteins expressed by two phytopathogens, *X. campestris* and *X. fastidiosa*, displayed the highest amino acid identity values, corresponding to 90 and 72% over the complete *X. citri* MBP amino acid sequence, respectively (Fig. 1A). Other MBP orthologs found in genomes of different bacterial species displayed significantly reduced identity values ranging from 20%, in *E. carotovora* to 9% in *S. flexneri* (Fig. 1A). Further computational analysis based on the presence of conserved structural and functional domains [14] revealed that the *X. citri* MBP shares high similarity values over most of the mature protein length with other periplasmic substrate binding proteins such as: SBP, a group of bacterial extracellular solute-binding proteins; UgpB, a group of proteins represented by the binding component of ABC-type sugar transport systems; MalE of MBP, the maltose and maltodextrin-binding proteins; and and PotD, formed by proteins with the ability to bind spermidine/putrescine (Fig. 1B). Thus, in spite of the low amino acid identity shared with previously identified orthologs, *X. citri* MBP preserves functional and structural domains, which are characteristic of periplasmic substrate binding proteins expressed by diverse gram-negative bacterial species.

Expression and purification of recombinant X. citri MBP

The recombinant MBP of *X. citri* was expressed and purified from *E. coli* BL21 as a soluble cytosolic protein (HT-MBP) genetically fused at the N-terminal end with a His_6-tag and an additional sequence (20 aa) defining thrombin cleavage site. Attempts to express the recombinant protein with an intact signal peptide and a C-terminal His_6-tag failed to promote secretion to the periplasmic space of the recombinant strain, suggesting that the *X. citri* MBP signal peptide was not recognized by the *E. coli* membrane protein secretion apparatus (data not shown). A putative 19 amino acid long MBP signal peptide was identified with the SignalP program. Specific primers were thus designed to amplify a 1.3 kbp fragment containing the *X. citri* mature MBP sequence to be cloned into the pET28a expression vector. The fragment was cloned in an intermediate vector (pGEM-T) before subsequent forced cloning into the *Nde*I and *Hin*dIII restriction sites of pET28a, which resulted in the pETMalE expression vector. The recombinant HT-MBP was expressed in *E. coli* BL21 under the control of the T7 phage promoter resulting in protein yields of approximately 100–150 mg/L, which corresponded to levels up to 40% of the total cell protein (Fig. 2). There is no evidence of growth impairment of bacterial colonies transformed with pETMalE under non-inducing conditions. However, a clear growth arrest was detected after addition of the inducer to the growth medium (data not shown). Different induction protocols based on variation of incubation temperature, aeration, culture media, and induction time were tested to optimize the expression yields of both total and soluble recombinant protein (Table 2). Under the tested conditions, maximal yields of the soluble protein were

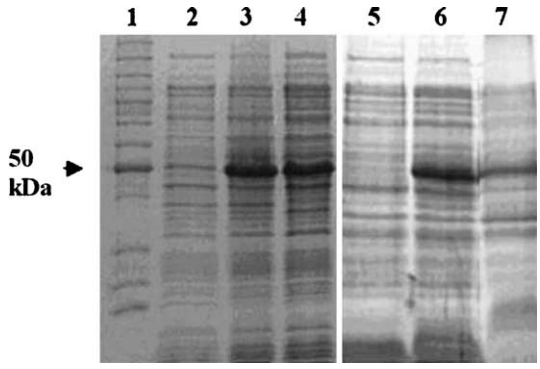

Fig. 2. Expression of recombinant HT-MBP in *E. coli* BL21(DE3). Whole-cell extracts or soluble fractions were loaded on polyacrylamide gels after IPTG induction in LB medium at 23 °C (lanes 2–4) or 37 °C (lanes 5–7). Lane 1, prestained molecular weight markers (Invitrogen); lanes 2 and 5, whole-cell extracts of non-induced cultures after overnight growth; lanes 3 and 6, whole-cell extracts of cultures kept overnight at the inducing conditions; and lanes 4 and 7, soluble fractions of cultures kept overnight at the inducing conditions. Similar protein amounts were loaded in each well (30 ng/well) and sorted in 12.5% polyacrylamide gels stained with Coomassie brilliant blue. The arrow indicates the position of the 50 kDa marker.

achieved in cultures prepared with LB medium kept overnight at 23 °C with low aeration levels, which resulted in an almost exclusively soluble protein at a concentration of 150 mg/ml (Table 2). Other tested conditions resulted in soluble recombinant protein at yields ranging from 91.5 to 26.6% of the total protein expressed (Table 2). For all conditions, the lack of aeration was an important factor for the observed increase in the solubility of the recombinant protein, particularly when the HT-MBP was induced at 28 °C. Similar high HT-MBP yields were obtained in cultures induced at 37 °C for 2 or 4 h when compared to samples incubated at lower temperatures for 16 h, but the solubility levels of the recombinant protein were clearly enhanced in cultures kept at 23 °C. Taken together, these data indicated that both aeration and induction temperature affect the expression of the recombinant protein, whereas conditions favoring reduced growth rates tended to enhance the solubility of the recombinant protein.

The protein was purified in a single step after elution of bound protein from loaded resin with imidazole-containing buffer at concentrations ranging from 50 to 150 mM (see Fig. 3A). Based on the elution carried out with 50 mM imidazole and cultures induced at 23 °C for 16 h in LB medium, the total recombinant protein yield ranged from 0.120 to 0.150 g/L. The purified protein remained completely soluble at high concentrations (15–30 mg/mL) even after prolonged storage at 4 or −20 °C. To evaluate the integrity and biological activity of the purified protein, the sugar-binding property of the recombinant HT-MBP was evaluated in binding assays carried out with an amylose-containing

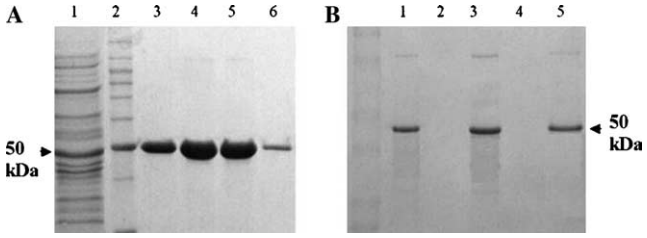

Fig. 3. Purification of HT-MBP and evaluation of amylose-binding property of the recombinant protein. (A) Purification of HT-MBP by affinity chromatography and elution with buffers containing different imidazole concentrations. Lane 1, flowthrough; 2, pre-stained molecular weight markers (Invitrogen); lanes 3–6, fractions eluted with buffers containing 50, 100, 200, and 500 mM imidazole, respectively. (B) Ligation of HT-MBP to amylose resin. The purified protein was mixed with the amylose resin at a 3:1 ratio and samples of the protein were analyzed by SDS–PAGE. Lane 1, purified MBP (1 μg); lane 2, amylose resin; lane 3, amylose + MBP; lane 4; flowthrough; and lane 5, MBP eluted with 150 mM maltose.

Table 2
Experimental conditions affecting recovery yields of both total and soluble recombinant HT-MBP

Induction temperature[a] (°C)	Aeration[b]	Culture media[c]	Induction period [d] (h)	Total protein[e] (g/L)	Soluble protein[f](g/L)	% Soluble protein[g]
37	+	LB	2	0.120	0.052	43.4
37	−	LB	4	0.110	0.064	58.2
37	+	M9	2	0.097	0.042	43.2
28	+	LB	2	0.126	0.073	58.0
28	−	LB	4	0.129	0.090	69.8
28	+	M9	2	0.120	0.032	26.6
28	−	M9	16	0.102	0.064	62.7
23	−	LB	16	0.150	0.150	100.0
23	−	M9	16	0.142	0.130	91.5

[a] Incubation temperature following addition of inducer to the bacterial culture, as described in the text.
[b] Cultures kept in flasks within an orbital shaker set at 200 rpm (+) or kept statically (−) during the induction period.
[c] LB, Luria broth, M9, M9 minimal salt medium.
[d] Cultures were kept under inducing conditions for 2 h, 4 h or overnight (16 h).
[e] Total protein yields as obtained with 1 L cultures kept in 3.6 L Fernbach flasks.
[f] Amount of soluble HT-protein recovered after affinity purification with nickel-charged resin and elution with imidazole-containing buffer.
[g] Ratio of recovered soluble protein (g/L)/ total protein (g/L) expressed in percentages.

resin. As shown in Fig. 3B, the purified MBP remained fully capable of binding the amylose resin, from which the protein was eluted with buffer containing 150 mM maltose. Such experimental evidence indicated that the purified HT-MBP remained biologically active, an indication of preserved conformation as compared with the native protein expressed by *X. citri*.

Maltose-binding studies of the purified recombinant X. citri MBP

Further evidence that the recombinant HT-MBP preserved the structure and biological function of the native *X. citri* MBP was obtained by determination of CD (Fig. 4A) and intrinsic emission fluorescence (Fig. 4B) spectra of the recombinant protein at unbound and maltose-bound states. The CD spectrum of HT-MBP (Fig. 4A) is characteristic of an α-helical protein with minima at 208 and 222 nm. The predicted secondary structure of the recombinant protein, carried out with the DICROPROT program, indicated an overall structure of the maltose-bound form of 36% α-helices and 17% β-strands, while turns and random coils represented 40% of the predicted secondary structure. These percentages are similar to that described for *E. coli* maltose-bound MBP (40% α-helices and 16% β-strand) [18]. The far-UV CD recorded spectra indicated that in the presence of maltose HT-MBP has a higher α-helical content than in the absence of maltose (Fig. 4A and Table 3). HT-MBP has 14 Trp residues and emission fluorescence spectroscopy was used to observe the environment of these residues (Fig. 4B). Since the observed fluorescence spectrum is a sum of each Trp fluorescence spectrum, only an average evaluation of the Trps environment is possible. The maximum intensity wavelength (λ_{max}) of fluorescence was 341 nm and the emission fluorescence center of mass was 354 nm (Table 3) indicating that, on average, the Trps were partially exposed to the solvent. There was also a detectable change in the HT-MBP emission fluorescence spectrum, which decreased in the presence of maltose as detected by the integer of the spectra (Table 3). However, this change was almost negligible inside the error.

Discussion

Plant bacterial pathogens, such as the *Xanthomonas* species, rely on the ability to promote the active transport of essential nutrients from infected tissues to thrive and proliferate, leading to disease symptoms in susceptible hosts. Maltose and maltodextrins (oligosaccharides up to 7 or 8 α-1,4-linked glucose units) are major polysaccharides available for bacteria in plant tissues, and represent important sources of carbon and energy. The uptake of maltose/maltodextrin in *E. coli* requires a

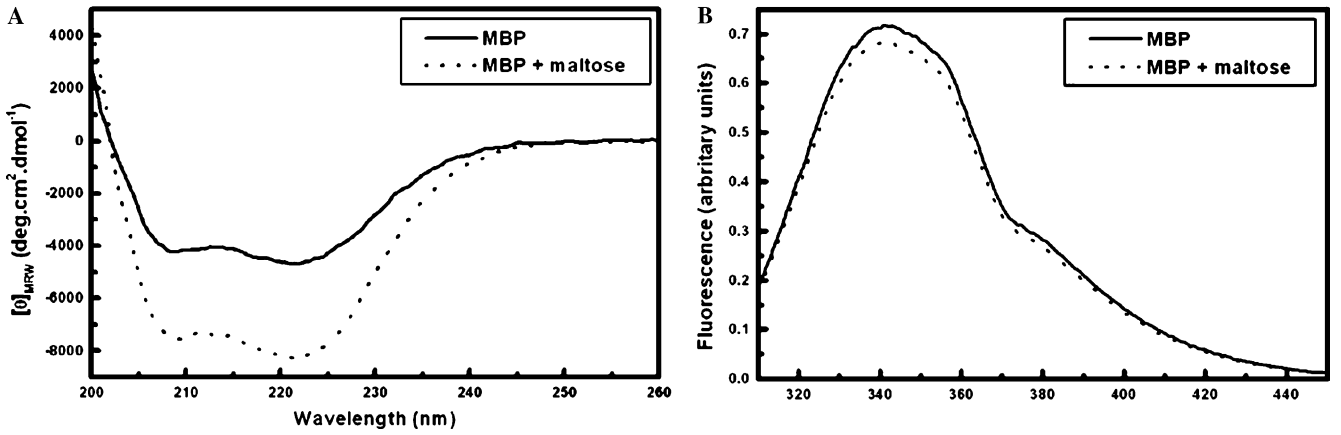

Fig. 4. CD and intrinsic fluorescence emission spectra of unbound and maltose-bound HT-MBP. (A) CD spectra of HT-MBP. The continuous line shows the spectrum acquired without adding ligand; the interrupted line represents the spectrum acquired in the presence of 20μM maltose. The spectrum of HT-MBP is characteristic of an α-helical protein. (B) Intrinsic emission fluorescence of the recombinant protein in the presence or absence of maltose. The solid line represents the emitted fluorescence of unbound HT-MBP while the interrupted line represents the emitted fluorescence of the protein in the presence of 9 μM maltose.

Table 3
HT-MBP spectroscopic parameters

Protein	CD at 222 nm (deg cm^2 dmol^{-1})	Fluorescence λ_{max}(nm)	Fluorescence center of mass (nm)	Fluorescence integer
MBP	−4700	341	354	43
MBP + maltose	−8300	341	354	41

Errors are less than 4%.

membrane-bound ABC-type transporter comprising two hydrophobic permeases (MalF and MalG), two copies of the ATPase subunit (MalK), and one binding protein (MBP or MalE), that confer specificity and affinity toward the transported solutes [1,19]. In spite of the obvious relevance of polysaccharide uptake systems in regard to understanding the nutritional strategies of plant pathogens, there has been no previous attempt to identify and characterize such proteins among *Xanthomonas* species. In this work, we describe the identification of the *X. citri* MBP-encoding gene and some of the properties of a recombinant protein while showing that both functional and conformational features of the protein are preserved.

Genes involved in maltose uptake have been identified in the annotated genomes of the plant pathogens *X. citri* and *X. campestris* [13]. In contrast to *E. coli* and other bacterial species, the genes encoding the binding component and the ATPase subunit of *X. citri* are not physically linked to those encoding the hydrophobic components, suggesting alternative regulatory pathways controlling the balanced expression of the transport system components. Moreover, comparison of the amino acid sequence of the *X. citri* maltose-binding component indicated that the protein, as well as those proteins derived from other plant pathogens (*X. campestris* and *X. fastidiosa*), has been engaged in a different phylogenetic branch. Despite the low similarity shared with orthologs expressed by other bacterial species, *X. citri* MBP possesses typical structural and functional domains of bacterial binding proteins involved in the active uptake of sugar and other nutrients, as demonstrated by the CD-Search program. The CD-Search multiple alignment tool supplies information on the presence of conserved conformational domains shared by groups of proteins displaying similar conformation and biological functions [14]. Taken together, these evidences suggest that *X. citri* MBP evolved distinctly from other orthologs yet preserving structural and functional features characteristic of ABC transporter ligand-binding components.

Attempts to express the *X. citri* MBP in recombinant *E. coli* strains have failed to promote secretion of the protein into the periplasmic space. Moreover, most of the expressed recombinant protein accumulated intracellularly as inclusion bodies. The *X. citri* MBP encompasses a mature polypeptide of 437 residues, including 47% non-polar, 28.8% uncharged polar, 12% acidic, and 12.2% basic amino acids, and a putative 19 amino acid long signal peptide. The failure to secrete the recombinant protein suggests that the secretion apparatus of *E. coli* does not efficiently recognize the signal sequence of *X. citri* MBP, an observation that could dictate further attempts to express *X. citri* secreted proteins. Nonetheless, successful expression of soluble MBP was achieved after removing the signal peptide and fusion of the His_6-tag to the N-terminal region. Using such approach, we could routinely attain high recovery yields of completely soluble *X. citri* MBP, which allowed purification of the recombinant protein at a nearly homogeneous state. The same strategy has been used to express other ABC transporter ligand-binding components and represents an experimental alternative to the expression of *X. citri* proteins to be purified by metal-affinity chromatography (unpublished observations).

The high solubility of HT-MBP and preserved ability to bind amylose suggest that *X. citri* MBP also represents a proper vehicle for the expression of target heterologous proteins in bacteria and eukaryotic systems. Previous comparison of different bacterial MBPs as fusion partners has indicated that proteins distantly related to the *E. coli* ortholog, such as those of *P. furiosus* and *T. litoralis*, can improve the solubility of recombinant heterologous proteins [20]. The successful expression of completely soluble MBP and the ability to purify protein through dual affinity chromatography point that further testing of *X. citri* MBP as a vehicle for expression of fused protein is worth pursuing.

The X-ray structures of *E. coli* maltose-free and maltose-bound MBP revealed that each monomer has two distinct globular domains separated by a groove wherein lies the ligand [4,21]. Upon maltose binding, a hinge bends repeatedly between the two globular domains, affecting the aromatic residues lining the binding cleft without significantly affecting the structure of the individual globular domains [4,21,22]. The aromatic residues involved in the hydrophobic interactions with the bound maltose are compressed against the sides of the binding cleft of the protein, restricting tryptophan, and tyrosine side chain mobilities, thus, reducing the static fluorescence emission of the protein [22]. Measurements of CD in the presence and absence of maltose confirmed that binding of maltose resulted in a large conformational change of the protein, most probably reflecting the movement of the two lateral domains toward the substrate buried inside the cleft. These data also confirmed that the purified recombinant protein preserved structural and functional features of the native protein expressed by *X. citri*.

Fluorescence enhancement appeared is usually dependent on conformational changes of proteins but static fluorescence measurements are limited in their ability to provide information on the specific amino acids and spatial movements involved. Sharff et al. [21], and Telmer and Shilton [7] showed that in *E. coli* the residues trp62, trp230, and trp340 are involved in hydrophobic stacking interactions with the bound maltose. The W230A mutation caused an increase in maltose-induced quenching to 30%, whereas the W158A mutation resulted in a complete loss of maltose-induced quenching [7]. In *X. citri* MBP, the trp230 and trp340

residues are conserved but the specific roles of such residues on the emitted fluorescence of the protein and ligand binding properties are still unknown. Further elucidation of MBP tri-dimensional structure will help in the general understanding of protein–ligand interactions and in the specific understanding of the putative roles of MBP on the physiology and pathogenicity of *X. citri*.

Acknowledgments

We thankfully acknowledge the helpful technical assistance of S.F.S. Lucas and continuous support of Dr. R. Meneghini. This work was supported by a FAPESP (Fundação de Amparo à Pesquisa do Estado de São Paulo) grant as part of the Structural and Molecular Biology Net Program (SMolBNet).

References

[1] W. Boos, H. Shuman, Maltose/maltodextrin system of *Escherichia coli*: transport, metabolism, and regulation, Microbiol. Mol. Biol. Rev. 62 (1998) 204–229.
[2] R. Tam, M.H. Saier, Structural, functional, and evolutionary relationships among extracellular solute-binding receptors of bacteria, Microbiol. Rev. 57 (1993) 320–346.
[3] J.A. Hall, K. Gehring, H. Nikaido, Two modes of ligand binding in maltose-binding protein of *Escherichia coli*, J. Biol. Chem. 272 (1997) 17605–17609.
[4] J.C. Spurlino, G.Y. Lu, F.A. Quicho, The 2.3A resolution structure of the maltose or maltodextrin-binding protein, a primary receptor of bacterial active transport and chemotaxis, J. Biol. Chem. 266 (1991) 5202–5219.
[5] F.A. Saul, M. Mourez, B.V. Le-Normand, N. Sassoon, G.A. Bentley, J.-M Betton, Crystal structure of a defective folding protein, Protein Sci. 12 (2003) 577–585.
[6] O. Millet, R.P. Hudson, L.E. Kay, The energetic cost of domain reorientation in maltose-binding protein as studied by NMR and fluorescence spectroscopy, Proc. Natl. Acad. Sci. USA 100 (2003) 12700–12705.
[7] P.G. Telmer, B.H. Shilton, Insights into the conformational equilibria of maltose-binding protein by analysis of high affinity mutants, J. Biol. Chem. 278 (2003) 34555–34567.
[8] Y. Zhang, P.J. Gardina, A.S. Kuebler, H.S. Kang, J.A. Christopher, M.D. Manson, Model of maltose-binding protein/chemoreceptor complex supports intrasubunit signaling mechanism, Proc. Natl. Acad. Sci. USA 96 (1999) 939–944.
[9] D. Wassemberg, W. Liebl, R. Jaenicke, Maltose-binding protein from the hyperthermophilic bacterium *Thermogota maritima*: stability and binding properties, J. Mol. Biol. 295 (2000) 279–288.
[10] J. Diez, K. Diederichs, G. Greller, R. Horlacher, W. Boos, W. Welte, The crystal structure of a liganded threalose/maltose-binding protein from hyperthermophilic archaeon *Thermococcus litoralis* at 1.85A, J. Mol. Biol. 305 (2001) 905–915.
[11] K. Schäfer, U. Magnusson, F. Scheffel, A. Schiefner, M.O.J. Sandgren, K. Diederichs, W. Welte, A. Hülsmann, E. Schneider, S. Mowbray, X-ray structures of the maltose-maltodextrin binding protein of the thermoacidophilic bacterium *Alicyclobacillus acidocaldarius* provide insight into acid stability of proteins, J. Mol. Biol. 335 (2004) 261–274.
[12] A.M. Brunings, D.W. Gabriel, *Xanthomonas citri*: breaking the surface, Mol. Plant Pathol. 4 (2003) 141–157.
[13] A.C da Silva, J.A. Ferro, F.C. Reinach, C.S. Farah, L.R. Furlan, R.B. Quaggio, C.B. Monteiro-Vitorello, M.A. Van Sluys, N.F. Almeida, L.M. Alves, A.M. do Amaral, M.C. Bertolini, L.E. Camargo, G. Camarotte, F. Cannavan, J. Cardozo, F. Chambergo, L.P. Ciapina, R.M. Cicarelli, L.L. Coutinho, J.R. Cursino-Santos, H. El-Dorry, J.B. Faria, A.J. Ferreira, R.C.C. Ferreira, M.I. Ferro, E.F. Formighieri, M.C. Franco, C.C. Greggio, A. Gruber, A.M. Katsuyama, L.T. Kishi, R.P. Leite, E.G. Lemos, M.V. Lemos, E.C. Locali, M.A. Machado, A.M. Madeira, N.M. Martinez-Rossi, E.C. Martins, J. Meidanis, C.F. Menck, C.Y. Miyaki, D.H. Moon, L.M. Moreira, M.T. Novo, V.K. Okura, M.C. Oliveira, V.R. Oliveira, H.A. Pereira, A. Rossi, J.A. Sena, C. Silva, R.F. de Souza, L.A. Spinola, M.A. Takita, R.E. Tamura, E.C. Teixeira, R.I. Tezza, M. Trindade dos Santos, D. Truffi, S.M. Tsai, F.F. White, J.C. Setubal, J.P. Kitajima, Comparison of the genomes of two *Xanthomonas* pathogens with differing host specificities, Nature 23 (2002) 459–463.
[14] A. Marchler-Bauer, S.H. Bryant, CD-Search: protein domain annotations on the fly, Nucleic Acid Res. 32 (2004) 327–331.
[15] H. Edelhock, Spectroscopic determination of tryptophan and tyrosine in protein, Biochemistry 6 (1997) 1948–1954.
[16] G. Deléage, C. Geourjon, An interactive graphic program for calculating the secondary structures content of proteins from circular dichroism spectrum, Comput. Appl. Biosc. 9 (1993) 197–199.
[17] J.L. Silva, E.W. Miles, G. Weber, Pressure dissociation and conformational drift of the β-dimer of tryptophan synthase, Biochemistry 25 (1986) 5780–5786.
[18] F.A. Quiocho, J.C. Spurlino, L.E. Rodseth, Extensive features of tight oligosaccharide binding revealed in high-resolution structures of the maltodextrin transport/chemosensory receptor, Structure 5 (1997) 997–1015.
[19] P. Duplay, H. Bedouelle, A. Fowler, I. Zabin, W. Saurin, M. Hofnung, Sequences of the *malE* gene and its product, the maltose-binding protein of *Escherichia coli* K12, J. Biol. Chem. 259 (1984) 10606–10613.
[20] J.D. Fox, K.M. Routzhan, M.H. Bucher, D.S. Waugh, Maltodextrin-binding proteins from diverse bacteria and archaea are potent solubility enhancers, FEBS Lett. 537 (2003) 53–57.
[21] A.J. Sharff, L.E. Rodseth, J.C. Spurlino, F.A. Quiocho, Crystallographic evidence of a large ligand-induced hinge-twist motion between the two domains of the maltodextrin binding protein involved in active transport and chemotaxis, Biochemistry 31 (1992) 10657–10663.
[22] G. Gilardi, G. Mei, N. Rosato, A.F. Agro, A.E.G. Cass, Spectroscopic properties of an engineered maltose binding protein, Protein Eng. 10 (1997) 479–486.